Biochemical and Biophysical Research Communications 445 (2014) 346–351

Contents lists available at ScienceDirect

Biochemical and Biophysical Research Communications

journal homepage: www.elsevier.com/locate/ybbrc

In vitro inhibition of fatty acid synthase by 1,2,3,4,6-penta-O-galloyl-β-D-glucose plays a vital role in anti-tumour activity

Wenhua Zhao, Yuji Wang, Weijia Hao, Ming Zhao *, Shiqi Peng *

Capital Medical University, 10 Xitoutiao, You An Men, Beijing 100069, PR China

ARTICLE INFO

Article history:
Received 29 January 2014
Available online 6 February 2014

Keywords:
1,2,3,4,6-Penta-O-galloyl-β-D-glucose (PGG)
Fatty acid synthase (FAS)
Anti-tumour

ABSTRACT

1,2,3,4,6-Penta-O-galloyl-β-D-glucose (PGG) inhibits glioma cancer U251 cells, more strongly than MDA-MB-231 and U87 cells. In addition, PGG is transported across cancer cell membrane to further down-regulate FAS and activate caspase-3 in MDA-MB-231 cells. Compared with other FAS inhibitors, including catechin gallate and morin, PGG involves a higher reversible fast-binding inhibition with half-inhibitory concentration value (IC_{50}) of 1.16 μM and an irreversible slow-binding inhibition, i.e. saturation kinetics with a dissociation constant of 0.59 μM and a limiting rate constant of 0.16 min^{-1}. The major reacting site of PGG is on the β-ketoacyl reduction domain of FAS. PGG exhibits different types of inhibitions against the three substrates in the FAS overall reaction. The higher concentrations of PGG tested (higher than 20 μM) clearly altered the secondary structure of FAS by increasing the α-helix and induced a redshift in the FAS spectra. In addition, only PGG concentrations higher than 20 μM resulted in FAS precipitation.

1. Introduction

Fatty acid synthase (FAS; EC 2.3.1.85) is highly expressed in certain human cancers [1,2] and is a potential target for cancer therapy [3,4]. The expression of FAS has been correlated with tumour metastasis [5,6] and has been found to have prognostic significance [7]. FAS inhibitors, both natural products and synthetic compounds, are receiving increasing attention due to their significant biological functions [8]. C75 is a synthetic FAS inhibitor with an IC_{50} of 58.7 μM for the FAS overall reaction [9]. However, the use of C75 *in vivo* is limited by its side effects, e.g., anorexia and body weight loss. Moreover, the inhibitors that are extracted from plants exhibit more efficient inhibitory activities than C75; these inhibitors have IC_{50} values in the range of 2.33–26.1 μM [10–12]. We have shown that by inhibiting FAS the extracts from *Acer* leaves significantly inhibit the growth of cancer cells [13,14]. To further investigate the major bioactive constituent, we have isolated 1,2,3,4,6-penta-O-galloyl-beta-D-glucose (PGG) from *Acer* leaves [15] and found that PGG inhibits FAS more effectively than all of the other studied compounds [16].

PGG (Fig. 1A) is one of the gallotannins that are generally found in various plants. It is noteworthy that a series of recent publications have demonstrated that PGG exhibits biological activities, including antibacterial activity [17], antiviral activity [18], anti-diabetes activity [19], anti-allergic activity [20] and *in vivo* anti-cancer efficacy [21–23]. However, because PGG is a hydrolysable tannin and its absorption and metabolism are not well elucidated, PGG is hypothesised to change into other metabolites and plays various roles in the plasma. A recent vital report showed that plasma PGG concentrations were approximately 3–4 μM in mouse [24]. The following pivotal questions in the field are whether PGG is transported across the membranes of cancer cells and whether its anti-tumour action is related to changes in the expression of the dominating protein in cancer cells.

In the present study, we evaluated the PGG-induced inhibition of FAS expression in breast and glioma cancer cells to determine whether PGG can be transported across cancer cells and whether PGG can change the expression of the dominating protein to influence apoptosis in cancer cells. The inhibitory effect of PGG on FAS, as well as the conformational changes in and the protein precipitation of FAS induced by PGG, were also investigated.

2. Materials and methods

2.1. Cell culture

The reagents were purchased from Gibco BRL. The human breast cancer MDA-MB-231 cells were maintained in RPMI 1640

Abbreviations: C, competitive inhibition; N, noncompetitive inhibition; U, uncompetitive inhibition.

* Corresponding authors. Fax: +86 10 8280 2482 (M. Zhao), +86 10 8391 1528 (S. Peng).

E-mail addresses: mingzhao@bjmu.edu.cn (M. Zhao), sqpeng@bjmu.edu.cn (S. Peng).

http://dx.doi.org/10.1016/j.bbrc.2014.01.191
0006-291X/

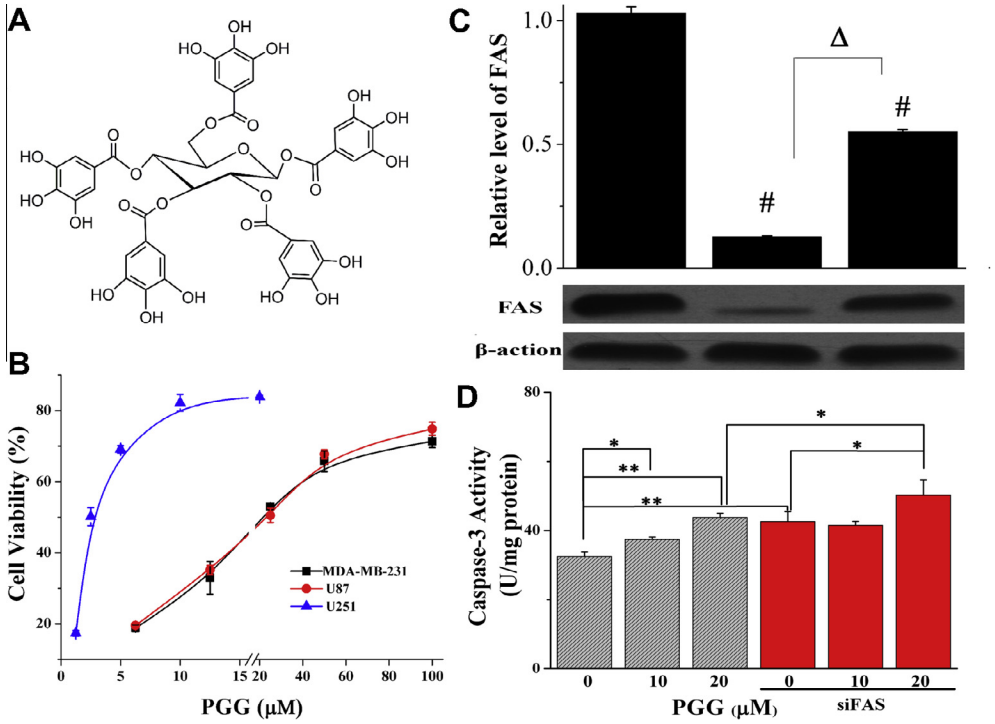

Fig. 1. Effect of PGG on cell viability and FAS expression in cancer cells. (A) Chemical structure of PGG. (B) The IC_{50} of PGG in U251 cells (2.5 μM) was tenfold lower than that (25 μM) in MDA-MB-231 and U87 cells. (C) Effect of PGG on FAS protein expression in MDA-MB-231 cells. After a 48-h incubation, the cells were treated with vehicle, 10 μM of PGG or 10 μM CG for 24 h. (D) Effect of PGG on caspase-3 in MDA-MB-231 cells with or without siFAS. The cells were treated with vehicle, 10 and 20 μM of PGG for 24 h and then harvested. All of the experiments were performed in triplicate.

medium containing 10% foetal bovine serum at 37 °C with 5% CO_2, whereas the glioma cancer U87 and U251 cells were maintained in DMEM medium under the same conditions.

2.2. Cell viability assay and caspase activity assay

The cancer cells were seeded in 96-well plates, and the cell viability was assayed with MTT method. Caspase-3 activity was measured according to the standard procedure of the caspase-3 activity assay kit.

2.3. Detection of PGG transport across cancer cells by MS spectra

After the MDA-MB-231cells were incubated with PGG for 3 days, the cells were extracted using the following procedure. The cells were grown in 75-cm^2 culture flasks, washed 3 times and then scraped into a tube containing 1 ml of ethyl acetate with 1% acetic acid. The tube was then shaken vigorously for 10 min and centrifuged at 5000 rpm for 5 min. A second extraction was performed by adding 1 ml of ethyl acetate to the tube containing the cells; the tube was then shaken for an additional 10 min and centrifuged again. The combined supernatant was dried through a Speedvac at 40 °C. The residue was dissolved in 200 μl of a solution composed of 50% methanol, 1% acetic acid water and 0.01% ascorbic acid and vortexed for 5 min. The solution was centrifuged at 16,000*g* for 10 min and filtered through a 0.45-μm filter. The supernatant was transferred to detect the formula weight using the MS spectra.

2.4. Western blotting

The MDA-MB-231 cells were treated with or without 10 μM PGG or 10 μM CG. The following antibodies were used: primary monoclonal antibody to FAS (1:2000 dilution; BD Transduction Laboratories) and anti-mouse IgG secondary antibody (1:2000 dilution).

2.5. Preparation and inhibition measurement of FAS

The purification and the inhibition assay of FAS were performed using previously described methods [13].

2.6. Measuring PGG-induced conformational change of FAS

The fluorescence emission spectra were measured using a Shimadzu RF-5301 fluorescence spectrophotometer with an excitation wavelength of 280 nm at 37 °C. The circular dichromism spectra were recorded on a Jasco 500C spectropolarimeter at 37 °C.

2.7. Measurement of protein precipitation induced by PGG

See Supplementary materials.

3. Results

3.1. PGG inhibits U251 cells more strongly than MDA-MB-231 and U87 cells

The effect of PGG on the growth of cancer cell was observed using MDA-MB-231, U87, and U251 cells. The treatment of the cells with serial dilutions of PGG in the range of 0.625–100 μM resulted in significant growth inhibition (Fig. 1B). In addition, the IC_{50} of PGG for U251 cells was 2.5 μM, which is significantly lower than the IC_{50} (25 μM) for MDA-MB-231 and U87 cells.

3.2. PGG inhibited FAS expression and activated caspase in MDA-MB-231 cells

The Western blotting results (Fig. 1C) show that FAS expression decreased significantly in both PGG-treated and the CG-treated MDA-MB-231 cells. A 24-h incubation with PGG inhibited FAS expression more strongly than a 24-h incubation with the same concentration of CG. The cleaved caspase-3 levels were significantly increased (Fig. 1D) suggested that the tumour cell killing by PGG was via activation of caspase-3.

3.3. PGG is transported across cancer cell membranes

PGG is transported across the membranes of cancer cells and plays a role in MDA-MB-231 cells. The structural identification of PGG was performed using its MS spectra. The MS spectra of the control cells that were not treated with PGG are shown in Fig. 2A. The MS spectra of the PGG solution without cells (the PGG control group), which are shown in Fig. 2B, exhibit an ESI-MS m/z of 939.2 (M−1), and the MS spectra of the PGG-treated cancer cells, which are shown in Fig. 2C, exhibit an ESI-MS m/z of 939.5 (M−1).

3.4. Fast-binding inhibition of FAS by PGG

PGG exhibited a concentration-dependent manner of the overall reaction of FAS, In addition, approximately 1.16 μM PGG inhibited 50% of the activity of FAS, whereas 2.5 μM PGG inhibited 50% of the acetoacetyl coenzyme A mediated reduction of FAS. In contrast, the inhibition of the enoyl reduction reaction was not clearly detected (Fig. 3A).

The inhibitions of FAS by PGG was measured and compared with that obtained with the same concentration of CG in the reaction system (Fig. 3B). The pre-incubation of PGG or CG with FAS for 30 min resulted in noticeable inhibitory effects. However, PGG exhibited more inhibition against FAS, as indicated by the measured residual activity of FAS after the incubation. The residual activities of FAS in cells treated with PGG and CG for 30 min were 32% and 21%, respectively, and the residual activities of FAS in cells treated with PGG and CG for 180 min were 18% and 10%, respectively (Fig. 3B).

The relevant kinetic mechanism for the inhibition of the overall reaction of FAS by PGG was estimated by maintaining the concentration of PGG at a set of fixed values and determining the effect that an increase in the concentration of one of the substrates on the initial reaction rate (Fig. 3C–F). The lineweaver–Burk plots of the overall reaction show that PGG is a typical competitive inhibitor of FAS against malonyl-CoA or NADPH. From the secondary plot of the slopes of these lines the inhibition constants (K_i) of 0.40 and 0.09 μM were obtained as a function of PGG concentration, respectively (Fig. 3C and D). However, the lines for acetyl-CoA as a function of PGG have a point of intersection in the second quadrant, which indicates that the type of inhibition was a mixture of competitive and noncompetitive (K_i = 0.43 μM, Fig. 3E). Moreover, the Lineweaver–Burk plot of the inhibition of β-ketoacyl reduction of FAS by PGG exhibited competitive inhibition against NADPH as the variable substrate for the KR of FAS (Fig. 3F), which was uniform for the overall reaction of FAS.

3.5. Time-dependent inactivation of FAS activity by PGG

PGG exhibited the capability to inactivate FAS activity in a time-dependent manner. The time courses of the inhibition of the overall reaction of FAS and the ketoacyl reduction reaction by 0.59 μM PGG are shown in Fig. 3G. The time courses show two distinct processes. The activity of FAS rapidly decreased by 40–50% in the first 3 min, this decrease was attributed to a fast and reversible binding of the substrate to the enzyme. The subsequent continued decrease in FAS activity appeared to be time-dependent and was irreversible due to the slow binding of PGG. The semilogarithmic plot of the

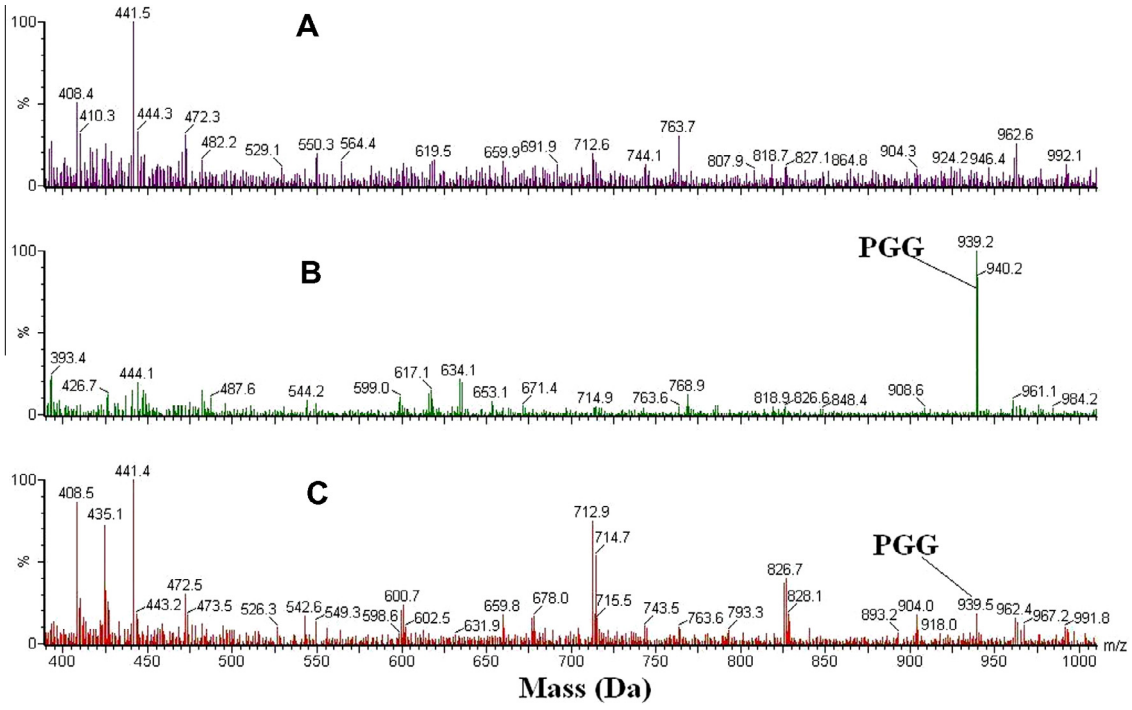

Fig. 2. ESI-MS of extracted MDA-MB-231 cells treated with PGG for 3 days. The following MS conditions were used: nitrogen gas 50 unit/min, spray voltage of 3.0 kV, capillary temperature of 275 °C and negative mode. The spectra of the following samples are shown: (A) cells not treated with PGG, (B) PGG solution without cells and (C) cells treated with PGG for 3 days.

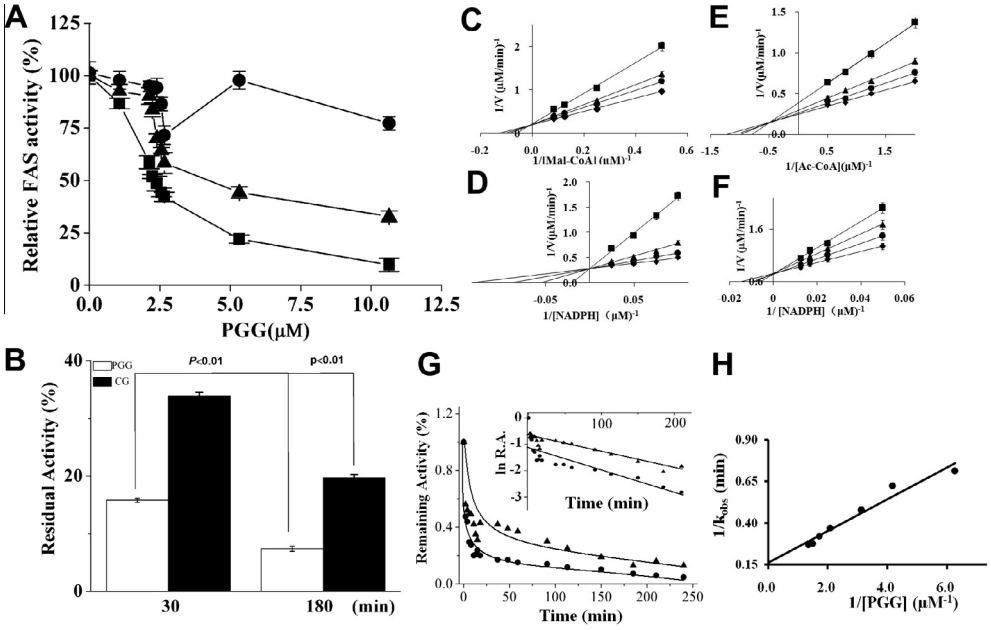

Fig. 3. Kinetic study of PGG on FAS. (A) Concentration-dependent inhibition of FAS by PGG: kinetics of the overall reaction (■), the ketoacyl reduction reaction (▲), and the enoyl reduction reaction (●) in the presence of PGG. The reaction system, which contains potassium phosphate buffer (0.1 M, pH 7.0), EDTA (1.0 mM), DTT (1.0 mM), acetyl-CoA (3 μM), malonyl-CoA (10 μM), NADPH (32 μM), and FAS (20 μg/2.0 ml) was maintained at 37 °C, and the NADPH was monitored at 340 nm for 1.5 min. (B) Comparison of the efficacy of the inhibition of FAS (1.9 μM) obtained with a 0.5- and 3.0-h incubation with PGG (1.25 μM) and CG (2.5 μM). The data are expressed as the mean ± SD. (C) Lineweaver–Burk plot of the inhibition of FAS by PGG. The concentrations of PGG in the overall reaction system were 0.00 M (♦), 0.59 μM (●), 0.88 μM (▲), and 1.17 μM (■). The fixed concentrations of NADPH and acetyl-CoA were 32 and 2.5 μM, respectively. (D) The fixed concentrations of malonyl-CoA and acetyl-CoA were 10 and 2.5 μM, respectively. (E) The fixed concentrations of NADPH and malonyl-CoA were 32 and 10 μM, respectively. (F) Lineweaver–Burk plot of the inhibition of the β-ketoacyl reduction reaction of FAS by PGG. The fixed concentration of ethyl acetoacetate is 40 mM, and the fixed concentrations of acetyl-CoA and malonyl-CoA were 2.5 and 10 μM, respectively. (G) Time course of the inhibition of the overall reaction (●) and the ketoacyl reduction reaction (▲) in the presence of PGG. The insert shows the semilogarithmic plot of the relative activity (ln R.A.) as a function of time. The FAS solution (0.60 μM) was mixed with PGG (0.59 μM), and aliquots were collected at the indicated time intervals to assay the remaining activity. (H) Effect of the concentration of PGG on the apparent inactivation rate constant, k_{obs}. The concentration of FAS in the inactivation system was 2.1 μM, and the plot shows the reciprocal of k_{obs} as a function of the reciprocal of the inhibitor (PGG) concentration.

relative activity (ln R.A.) as a function of time (insert of Fig. 3G) shows these two processes more clearly. This plot, which is first concave and then linear, was used to determine the inactivation rate constant (k_{obs}), which was equal to the fitted slope of the plots. The k_{obs} values of the inactivation of the overall reaction and the ketoacyl reduction reaction by PGG were 0.0083 and 0.0062 min^{-1}, respectively. It was shown that the rate of inactivation of the overall reaction was approximately 1.2-fold higher than that of the ketoacyl reduction reaction. The concentration-dependent plot of k_{obs} as a function of the concentration of PGG is shown in Fig. 3H. The hyperbola demonstrated the two-step reaction sequence for affinity labelling. First, PGG reversibly associates with the enzyme to form an enzyme–inhibitor complex (E–I). This complex then undergoes an irreversible chemical modification. K_s is the apparent half-saturation constant, which is the dissociation constant of E–I, where k (the first-order rate constant) is rate-limiting. The reciprocal of the plot of $1/k_{obs}$ as a function of 1/[PGG] is linear, and a K_s value of 0.59 μM and a k value of 0.16 min^{-1} were calculated from Fig. 3H.

3.6. FAS conformational changes induced by PGG

The CD spectra of the enzyme in different concentrations of PGG are shown in Fig. 4A. The lower concentrations (less than 10 μM) of PGG appreciably affect the secondary structure of FAS, and 10 μM PGG exhibited the most ability to affect the secondary structure. The higher concentrations (higher than 20 μM) of PGG clearly change the secondary structure of FAS by increasing the α-helix of FAS. A concentration of PGG between 10 and 20 μM slightly increased the α-helix.

Fig. 4B–D shows the fluorescence emission spectra of FAS with PGG at different concentrations. Although the peak value did not change with different concentrations of PGG, increasing concentrations of PGG decreased the fluorescence emission to its minimum, which was obtained with 30 μM PGG. A slight redshift was observed when the concentration of PGG was higher than 20 μM, and the synchronous fluorescence spectra show the same results.

4. Discussion

By being transported across membrane, PGG targets FAS, down-regulates the expression of FAS, inhibits the overall reaction and the ketoacyl reduction of FAS, and consequently cures cancer. Low concentrations (less than 20 μM) of PGG cannot induce conformational changes nor the precipitation of FAS.

In vivo PGG exhibits anti-cancer effects through various mechanisms, including pro-apoptosis, anti-proliferation, anti-angiogenesis, anti-metastasis, decrease of pSTAT3 and pJAK1, induction of SHP1 expression, down-regulation of cyclo-oxygenase-2 and VEGF as well as the inhibition of P-glycoprotein and DNA polymerases [23–26]. The glioma cancer cell lines U251 and U87 and the breast cancer cell line MDA-MB-231 express these higher concentrations of FAS [2,3]. It is noteworthy that, of these three cell lines, U251 cells express the highest FAS concentration [2]. We found that PGG inhibits U251 cells more strongly than MDA-MB-231 and U87 cells, which express lower concentrations of FAS than U251 cells. This finding initially demonstrates that PGG can be used to target FAS in cancer therapy. FAS down-regulation and caspase-3 activation were observed in PGG treated MDA-MB-231 cells, further suggesting PGG targets FAS in cancer cells. The speciality of

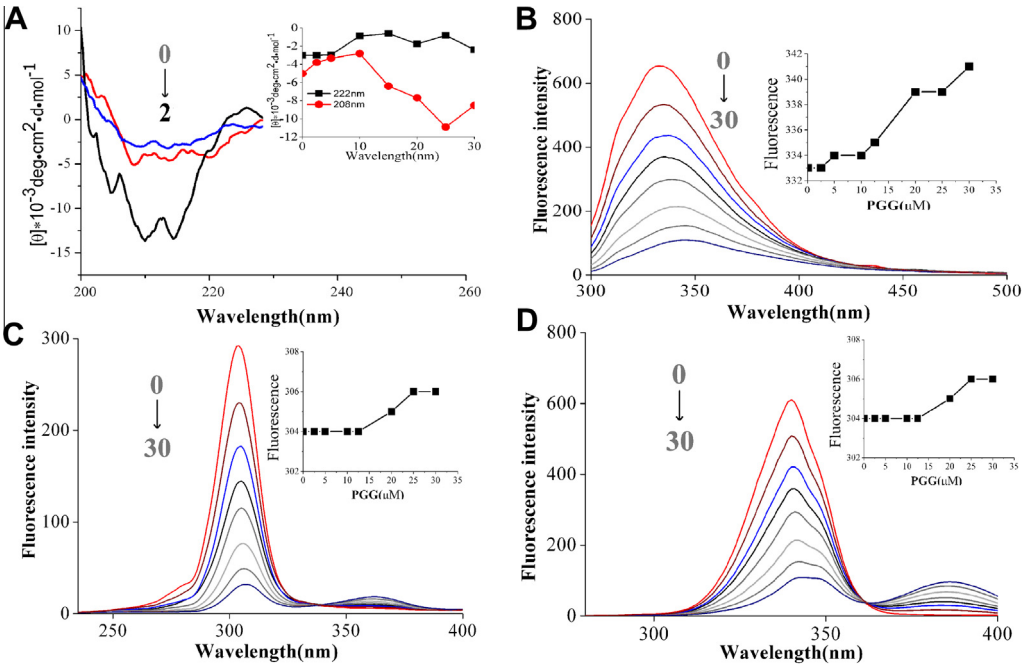

Fig. 4. Conformational changes in FAS induced by PGG. (A) CD spectra of FAS in the presence of PGG. The final concentrations of PGG used to obtain curves 0 through 2 were 10, 0 and 25 μM, respectively. (B) Concentration-dependent effect of PGG (0, 2.5, 5.0, 10, 15, 20, 25 and 30 μM) on the fluorescence intensity of FAS (1.0 μM) after a 10-min incubation. The fluorescence spectra was obtained with λ_{ex} = 280 nm. (C) Synchronous fluorescence spectra ($\Delta\lambda$ = 60 nm) obtained with λ_{ex} = 220 nm. (D) Synchronous fluorescence spectra ($\Delta\lambda$ = 15 nm) obtained with λ_{ex} = 220 nm and T = 310 K.

PGG being transported across cancer cell membrane is consistent with previously reported finding that PGG can be transported across the membrane of Caco-2 cells [27].

The IC_{50} of PGG on the overall reaction of FAS is 1.16 μM (Fig. 3A) and lower than that of the previously identified inhibitors such as morin (2.33 μM [8]) and catechin gallate (CG, 3.4 μM [10]), indicating that PGG may exhibit higher effectiveness compared with the previously identified inhibitors. The comparison results shown in Fig. 3B, which demonstrate that PGG exhibits a stronger inhibition against FAS compared with CG, further support the conclusion that PGG is the most effective inhibitor found to date. The fact that the core structure of PGG contains a galloyl structure is consistent with a report that found that the galloyl moiety is a critical structural feature for the inhibition of FAS [28]. PGG rapidly associates with FAS to exhibit fast-binding inhibition and then irreversibly inactivates FAS until the enzyme loses all of its activity. The inhibition by PGG exhibits the saturation kinetics behaviour typical of affinity labelling. Of note, the inhibitory characteristics of PGG were different from those of CG and morin (see Table 1). CG inhibits FAS competitively against acetyl-CoA. Morin inhibits the FAS overall reaction competitively against acetyl-CoA, noncompetitively against malonyl-CoA, and in a mixed competitive and noncompetitive manner against NADPH [28]. In contrast, PGG acts as a competitive inhibitor of FAS against malonyl-CoA and NADPH. This feature makes PGG a novel and potent inhibitor of FAS, which will prove helpful for the achievement of a cooperative effect between the components of the FAS reaction and thus deserves further in-depth study. Because FAS has been found to be a potential target for cancer therapy, the cooperative inhibition between PGG and other inhibitors, such as morin and CG, may improve cancer therapies in the future.

At a concentration of less than 10 μM PGG obviously inhibited FAS activity, and did not change the secondary structure of FAS, demonstrating that at lower concentration PGG decreased the activity of FAS only through competition with the active domains. Concentrations of PGG between 10 and 20 μM decreased the activity of FAS duo to a competitive effect and conformational regulation. However, the effect of PGG concentrations higher than 20 μM involves conformational changes in the structure of FAS and the precipitation of FAS (Supplementary materials). The concentrations of PGG inducing FAS to precipitate are at least 20-fold higher than the IC_{50}, providing a base for the safe use of PGG in chemotherapy.

Table 1
Inhibition type and inhibition constants for the overall reaction of FAS obtained with PGG, CG and Morin.

Substrate	PGG		CG[10]		Morin[28]	
	Type	K_i (μM)	Type	K_i (μM)	Type	K_i (μM)
Acetyl-CoA	C + N	0.43	C	0.49	C	3.57
Malonyl-CoA	C	0.40	N	0.92	N	2.46
NADPH	C	0.09	C + N	1.87	C + N	2.05

Acknowledgments

This work was supported by Grant 7112016 of the Natural Science Foundation of Beijing and Grant 21201124 of the National Science Foundation of China. Thanks for the support of Engineering Research Center of Endogenious Preventive Drug, Beijing Key Laboratory of Peptide and Small Molecule Drug and The Project of Construction of Innovative Teams and Teacher Career Development for Universities and Colleges Under Beijing Municipality and The Youth Talent and Science commission of Municipal Education Commission of Beijing.

Appendix A. Supplementary data

Supplementary data associated with this article can be found, in the online version, at http://dx.doi.org/10.1016/j.bbrc.2014.01.191.

References

[1] T. Maier, M. Leibundgut, N. Ban, The crystal structure of a mammalian fatty acid synthase, Science 321 (2008) 1315–1322.

[2] L.Z. Milgraum, L.A. Witters, G.R. Pasternack, F.P. Kuhajda, Enzymes of the fatty acid synthesis pathway are highly expressed in situ breast carcinoma, Clin. Cancer Res. 3 (1997) 2115–2120.

[3] F.P. Kuhajda, Fatty acid synthase and cancer: new application of an old pathway, Cancer Res. 66 (2006) 5977–5980.

[4] R. Flavin, S. Peluso, P.L. Nguyen, M. Loda, Fatty acid synthase as a potential therapeutic target in cancer, Future Oncol. 6 (2010) 551–562.

[5] J.V. Swinnen, T. Roskams, S. Joniau, H. Van Poppel, R. Oyen, L. Baert, W. Heyns, G. Verhoeven, Overexpression of fatty acid synthase is an early and common event in the development of prostate cancer, Int. J. Cancer 98 (2002) 19–22.

[6] P. Visca, V. Sebastiani, C. Botti, M.G. Diodoro, R.P. Lasagni, F. Romagnoli, A. Brenna, B.C. De Joannon, R.P. Donnorso, G. Lombardi, P.L. Alo, Fatty acid synthase (FAS) is a marker of increased risk of recurrence in lung carcinoma, Anticancer Res. 24 (2004) 4169–4173.

[7] T. Migita, S. Ruiz, A. Fornari, M. Fiorentino, C. Priolo, G. Zadra, F. Inazuka, C. Grisanzio, E. Palescandolo, E. Shin, C. Fiore, W. Xie, A.L. Kung, P.G. Febbo, A. Subramanian, L. Mucci, J. Ma, S. Signoretti, M. Stampfer, W.C. Hahn, S. Finn, M. Loda, Fatty acid synthase: a metabolic enzyme and candidate oncogene in prostate cancer, J. Natl. Cancer Inst. 101 (2009) 519–532.

[8] W.X. Tian, Fatty acid synthase by polyphenols, Curr. Med. Chem. 13 (2006) 967–997.

[9] T.M. Loftus, D.E. Jaworsky, G.L. Frehywot, C.A. Townsend, G.V. Ronnett, M.D. Lane, F.P. Kuhajda, Reduced food intake and body weight in mice treated with fatty acid synthase inhibitors, Science 288 (2000) 2379–2381.

[10] R. Zhang, W.P. Xiao, X. Wang, X.D. Wu, W.X. Tian, Novel inhibitors of fatty-acid synthase from green tea (*Camellia sinensis* Xihu Longjing) with high activity and a new reacting site, Biotechnol. Appl. Biochem. 43 (2006) 1–7.

[11] S.Y. Zhang, C.G. Zheng, X.Y. Yan, W.X. Tian, Low concentration of condensed tannins from catechu significantly inhibits fatty acid synthase and growth of MCF-7 cellsm, Biochem. Biophs. Res. Commun. 371 (2008) 654–658.

[12] X.B. Sun, W.X. Tian, Inhibitory effects of allium vegetable extracts on fatty acid synthase, Food Sci. Technol. Res. 15 (2009) 343–346.

[13] W.H. Zhao, J.F. Zhang, Z. Wang, Y.X. Zhang, W.X. Tian, The extract of leaves of *Acer truncatum Bunge*: a natural inhibitor of fatty acid synthase with antitumor activity, J. Enzyme Inhib. Med. Chem. 21 (2006) 589–596.

[14] W.H. Zhao, Ch.Ch. Gao, Y.X. Zhang, W.X. Tian, Evaluation of the inhibitory activities of aceraceous plants on fatty acid synthase, J. Enzyme Inhib. Med. Chem. 22 (2007) 501–510.

[15] W.H. Zhao, Ch.Ch. Gao, X.F. Ma, X.Y. Bai, Y.X. Zhang, The isolation of 1,2,3,4,6-penta-O-galloyl-beta-D-glucose from *Acer truncatum* Bunge by high-speed counter-current chromatography, J. Chromatogr. B 850 (2007) 523–527.

[16] W.H. Zhao, L.F. Gao, W. Gao, Y. Sh. Yuan, Ch.Ch. Gao, L.G. Cao, Z.Z. Hu, J.X. Guo, Y.X. Zhang, Weight reducing effect of *Acer truncatum* Bunge may be related to the inhibition of fatty acid synthase, Nat. Prod. Res. 25 (2011) 422–431.

[17] J.Y. Cho, M.J. Sohn, J.K. Lee, W.G. Kim, Isolation and identification of pentagalloylglucose with broad-spectrum antibacterial activity from *Rhus trichocarpa* Miquel, Food Chem. 123 (2010) 501–506.

[18] Y. Pei, Z.P. Chen, H.Q. Ju, M. Komatsu, Y. Ji, G. Liu, C.W. Guo, Y.J. Zhang, C.R. Yang, Y.F. Wang, K. Kitazato, Autophagy is involved in anti-viral activity of pentagalloylglucose (PGG) against Herpes simplex virus type 1 infection *in vitro*, Biochem. Biophs. Res. Commun. 405 (2011) 186–191.

[19] J. Lee, D.S. Jang, N.H. Kim, Y.M. Lee, J.H. Kim, J.S. Kim, Galloyl glucoses from the seeds of *Cornus officinalis* with inhibitory activity against protein glycation, aldose reductase, and cataractogenesis ex vivo, Biol. Pharm. Bull. 34 (2011) 443–446.

[20] K.Y. Natsuko, S. Yoko, M. Futoshi, K. Shun-ichiro, F. Junya, K. Tatsuo, Y. Takeshi, K. Makoto, Pentagalloylglucose down-regulates mast cell surface $Fc_{\varepsilon}RI$ expression *in vitro* and *in vivo*, FEBS Lett. 584 (2010) 111–118.

[21] J.H. Zhang, L. Li, S.H. Kim, A.E. Hagerman, J.X. Lü, Anti-cancer, anti-diabetic and other pharmacologic and biological activities of penta-galloyl-glucose, Pharm. Res. 26 (2009) 2066–2079.

[22] H.B. Hu, Y.B. Chai, L. Wang, J.H. Zhang, H.J. Lee, S.H. Kim, J.X. Lu, Pentagalloylglucose induces autophagy and caspase-independent programmed deaths in human PC-3 and mouse TRAMP-C2 prostate cancer cells, Mol. Cancer Ther. 8 (2009) 2833–2843.

[23] H.J. Lee, N.J. Seo, S.J. Jeong, Y.J. Park, D.B. Jung, W.H. Koh, H.J. Lee, E.O. Lee, K.S. Ahn, K.S. Ahn, J. Lü, S.H. Kim, Oral administration of penta-O-galloyl-β-D-glucose suppresses triple-negative breast cancer xenograft growth and metastasis in strong association with JAK1-STAT3 Inhibition, Carcinogenesis 32 (2011) 804–811.

[24] L. Li, A.A. Shaika, J.H. Zhang, K. Nhkata, L. Wang, Y. Zhang, C.G. Xing, S.H. Kim, J.X. Lü, Preparation of penta-O-galloyl-beta-D-glucose from tannic acid and plasma pharmacokinetic analyses by liquid–liquid extraction and reverse-phase HPLC, J. Pharm. Biomed. Anal. 54 (2011) 545–550.

[25] J.E. Huh, E.O. Lee, M.S. Kim, K.S. Kang, C.H. Kim, B.C. Cha, Y.J. Surh, S.H. Kim, Penta-O-galloyl-beta-D-glucose suppresses tumor growth via inhibition of angiogenesis and stimulation of apoptosis: roles of cyclooxygenase-2 and mitogen-activated protein kinase pathways, Carcinogenesis 26 (2005) 1436–1445.

[26] M. Yoshiyuki, J.H.i. Zhang, A. Pugliese, S.H. Kim, J. Lu, Anti-cancer gallotannin pentaglucose is a nanomolar inhibitor of select mammalian DNA polymerases, Biochem. Pharmacol. 80 (2010) 1125–1132.

[27] K. Cai, A.E. Hagerman, R.E. Minto, A. Bennick, Decreased polyphenol transport across cultured intestinal cells by a salivary proline-rich protein, Biochem. Pharmacol. 71 (2006) 1570–1580.

[28] X. Wang, K.S. Song, Q.X. Guo, W.X. Tian, The galloyl moiety of green tea catechins is the critical structural feature to inhibit fatty-acid synthase, Biochem. Pharmacol. 66 (2003) 2039–2047.